

Effects of annealing on the magnetoresistance and structure of Fe/Cr(110) superlattices

Jose M. Colino* and Ivan K. Schuller

Physics Department 0319, University of California at San Diego, La Jolla, California 92093-0319

V. Korenivski and K. V. Rao

Department of Condensed Matter Physics, Royal Institute of Technology, 10044 Stockholm, Sweden

(Received 28 August 1995; revised manuscript received 29 February 1996)

We have performed magnetotransport, magnetization, and structural experiments on sputtered Fe(30 Å)/Cr(12 Å) (110) superlattices that were annealed at temperatures up to 400 °C. Interestingly, their giant magnetoresistance ($\Delta\rho$) is enhanced at intermediate temperatures, and strongly decreased at higher temperatures. If normalized to the antiferromagnetic coupling fraction of sample, the magnetoresistance increases over the entire annealing range. From low-angle x-ray-diffraction measurements, the enhancement of $\Delta\rho$ arises from an interface redistribution because of either a slight interdiffusion, less correlated interfaces, or both. Further annealing causes extreme interdiffusion that is detrimental for the magnetoresistance because of a loss of antiferromagnetic coupling. [S0163-1829(96)01642-6]

Giant magnetoresistance (GMR) in artificial magnetic/normal multilayers has attracted much recent attention.¹ Experimental and theoretical work have revealed many of basic ingredients of the GMR, including the interplay of interlayer antiferromagnetic (AF) coupling² with spin-dependent electron scattering,³ the role of the type of elements in the layers, the crystalline structure,^{2,4} etc. However, a satisfactory overall model connecting physical and electronic structure with GMR has not yet emerged. For instance, the role of the spacers' electronic structure is strongly debated.⁴⁻⁶ Another critical issue is the coupling between magnetic layers. The importance of the Ruderman-Kittel-Kasuya-Yosida interaction compared to others such as the classical dipolar interaction⁷ caused by interface roughness, is still unclear. In this regard, the roughness and interface structure has been shown to be important factors for increasing the GMR.⁸⁻¹⁰ To date several approaches have been successfully used to enhance the GMR ($=\Delta\rho/\rho$) or $\Delta\rho$ to some extent. Interface roughness can be induced during growth by changing the deposition parameters, for instance by increasing Ar sputtering pressures.^{8,11} This way, the GMR of Fe(30 Å)/Cr(18 Å) (110) at 10 K was increased from ~ 6 to $\sim 13\%$.⁸ The interface structure can also be altered during growth and the GMR dramatically increased by addition of thin Co interface layers in Ni₈₁Fe₁₉/Cu multilayers.¹² Post-deposition Xe⁺ ion irradiation of Fe/Cr(110) changes the GMR in a controlled fashion.¹³ A reproducible method, which may be of technological importance, is simple annealing in vacuum or inert gases. Petroff *et al.* reported GMR increases from 14 to 27.3 % at helium temperature by annealing an Fe/Cr(100) sample at 300 °C for 1 h, and speculated that this was caused by changes in the interface roughness and scattering.¹⁰ Thermal treatments produce structural changes both at interfaces and in the bulk of multilayers, including chemical interdiffusion,¹⁴ changes in crystallinity, etc., which can be studied with x-ray diffraction.¹⁵

In this paper, we present a systematic study of structure and GMR in Fe/Cr(110) annealed at an inert gas atmosphere (Ar, He) for 30 min or 12 h. Magnetotransport experiments

show a significant enhancement of GMR at intermediate temperatures 150 °C, 12 h and 300 °, 30 min), and at all temperatures if normalized to the antiferromagnetic coupling fraction of the samples. The x-ray diffraction indicates changes in the interface structure at the annealing temperatures for greatest GMR.

[Fe(30 Å)/Cr(12 Å)]₁₀ (110) multilayers were grown at room temperature on Si(100) wafers by dc magnetron sputtering in a 4 mTorr argon atmosphere. Further deposition details have been reported elsewhere.⁸ The samples's structure was characterized by high- and low-angle x-ray diffraction using a Rigaku rotating anode diffractometer with Cu $K\alpha$ radiation, in specular and off-specular scans (rocking curves). Four lead magnetotransport measurements were performed at 4.2 and 77 K and magnetic fields up to 5 T. The magnetic field was in the film plane and perpendicular to the dc electrical current. The absolute value of the resistivity was determined either by the Van der Pauw method or directly using photolithographically patterned samples. The magnetization was measured by superconducting quantum interference device magnetometry at 10 K.

Two different thermal treatments were performed. In the first one, the sample is annealed at 100 °C for 30 min, then cooled to low temperatures and the magnetic and transport properties measured. Then the sample is annealed at 150 °C for 30 min, after which magnetic and transport properties are measured again. This procedure is repeated several times, increasing the annealing temperature by 50 °C at every step, up to an annealing temperature of 450 °C. Heating and cooling rates were greater than 40 °C/min. In the second method, the as-prepared film was cut into several samples. Each sample was annealed once at a single temperature in the range 100–400 °C for 12 h (heating/cooling rates=10 °C/min). Structural and magnetotransport measurements followed the annealings. The first method is well suited for following the process in one sample, although the effect is cumulative, and the second is useful to study temperature dependences.

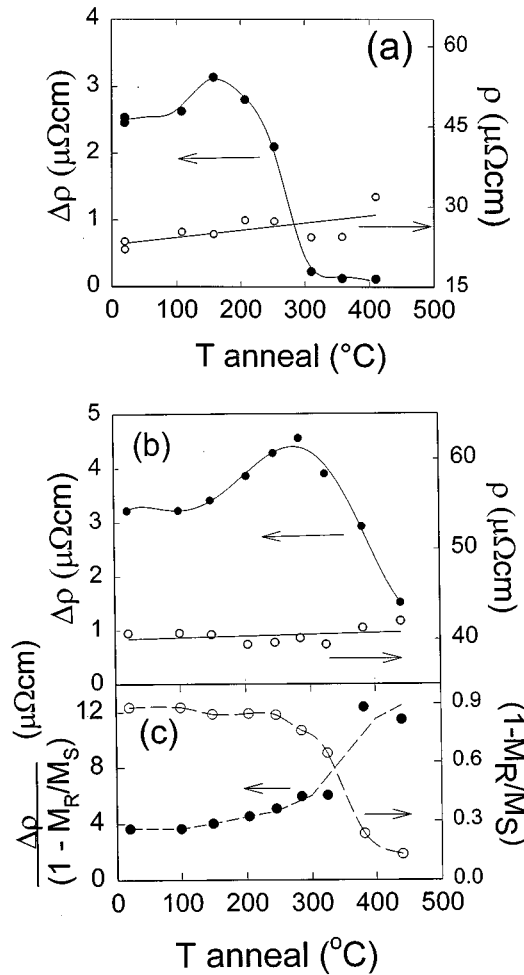


FIG. 1. $\Delta\rho$ and ρ versus annealing temperature for (a) 12 h annealed pieces of a single sample and (b) one sample annealed in 30 min steps. The two data at room temperature (a) are measurements on different pieces to check the reproducibility. (c) Magnetoresistance normalized to the AF coupling fraction of sample for the multilayer annealed in 30 min steps, and the AF coupling fraction of sample ($1 - M_R/M_S$). Saturation magnetization (M_S) is typically 1200 emu/cc, about 70% of the bulk M_S value. The lines are guides to the eye.

Figures 1(a) and 1(b) show the magnetoresistance at 4.2 K ($\Delta\rho$) and the saturation resistivity (ρ) as a function of annealing temperature for the two types of heat treatments described above. Whereas the resistivity exhibits a slight *monotonic* increase in the 20–420 °C range, $\Delta\rho$ shows an interesting *nonmonotonic* behavior; it rises to a maximum at intermediate temperatures (around 300 °C, 30 min and 150 °C, 12 h), increasing over initial values of as-prepared samples by 50% (a) and 28% (b), respectively, and thereafter drops to very small values. Actual values of $\Delta\rho/\rho$ are $\sim 8\%$ (a) and $\sim 10\%$ (b) for as-prepared samples, and upon annealing they reach $\sim 11.2\%$ (a) and $\sim 12.2\%$ (b) at the maximum. This increase of $\Delta\rho$ is the main focus of this paper.

To distinguish the effects of changing coupling behavior from more intrinsic effects, we have estimated the fraction of sample which is antiferromagnetically coupled

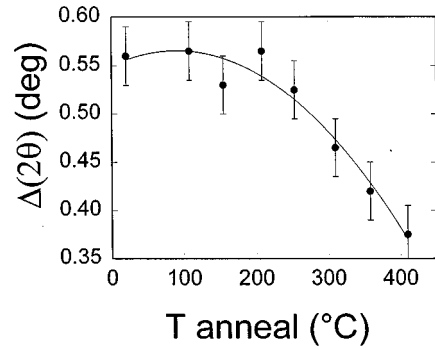


FIG. 2. Full width at half maximum (FWHM) of the $\theta-2\theta$ (110) peak of the 12h annealed samples [$\Delta(2\theta)$]. The lines are guides to the eye.

($1 - M_R/M_S$), where the giant spin-dependent scattering is localized, and plotted the magnetoresistance normalized to such a fraction. Figure 1(c) shows a steady increase of normalized GMR over all the temperature range tested for samples annealed for 30 min. This shows that the enhancement is even more important at higher temperatures and that the decrease of $\Delta\rho$ [Figs. 1(a) and 1(b)] is caused by a progressive loss of antiferromagnetic order due to magnetic shorts. Since the chemical interdiffusion in Fe/Cr (110) multilayers is significant at 350 °C for 3 h,¹⁴ interdiffusion is a likely explanation for our results above 300 °C (1/2 h).

High- and low-angle specular and nonspecular (rocking curves) x-ray-diffraction measurements were carried out for the 12 h annealed samples. As-prepared and annealed samples showed one first-order superlattice peak in the high-angle spectra about the (110) Bragg reflection. Full widths at half maximum (FWHM) of the (110) reflection are plotted in Fig. 2 versus annealing temperature. Above 200 °C, there is a remarkable decrease of the specular peak width [Fig. 3(b)] that, according to Scherrer's formula, corresponds to an enlargement of the average crystallite size (~ 240 Å) by a factor of ~ 1.6 over that of the as-grown sample (~ 150 Å), perhaps resulting from bulk defect annihilation, decrease of atomic strain, etc. Nearly constant rocking curve widths, about the (110) reflection (15° – 17°), imply minimal changes in crystalline orientation during annealing.

Figure 3 shows low-angle x-ray diffraction (LAXRD) specular spectra for the 12 h annealed samples. Up to third-order superlattice Bragg peaks confirm the multilayer periodicity of 42 Å repeated 10 times. An important result is that, even up to 350 °C, these low-angle spectra exhibit finite size and well developed Bragg peaks similar to those of the as-prepared samples.

Figure 4(a) shows the ratio of intensity of second-order ($n=2$) superlattice peaks over the background intensity, from $\theta-2\theta$ scans (Fig. 3), as a function of annealing temperature. We chose the second-order peaks since the finite-size peaks around it are small and thus allow a more precise determination of the background level. The decrease in Bragg peak intensities without broadening, for annealing temperatures above 100 °C, implies an increased interdiffusion.^{15,16}

Further insight from LAXRD can be gained by studying

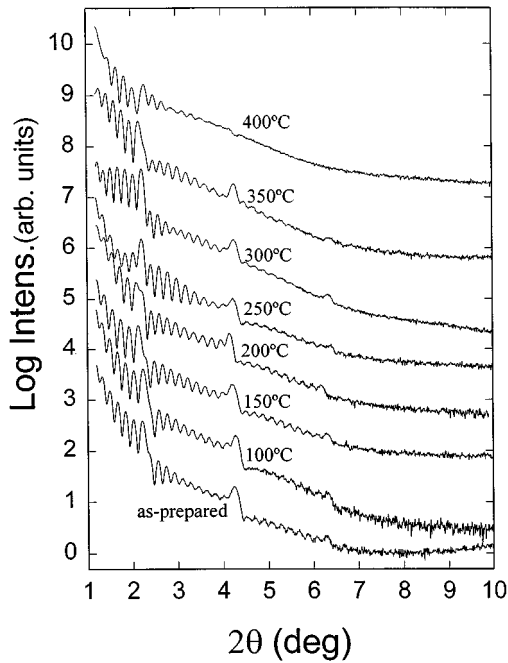


FIG. 3. Low-angle specular spectra of the as-prepared and annealed samples (for 12 h). The spectra are offset for clarity. Note the well developed finite-size peaks up to $\sim 350^\circ\text{C}$.

off-specular diffraction (rocking curves) at low-angle superlattice reflections. This diffusion scattering results from in-plane structural inhomogeneities associated with the individual interfaces or layers.^{17,18} In principle, diffuse scattering arises from vertically correlated and uncorrelated roughness. Correlated roughness, i.e., interfacial roughness replicated from layer to layer, originates from defects in the substrate or is due to growth front effect which give correlations in film morphology. Uncorrelated roughness is random from layer to layer. The inset of Fig. 4(b) shows the specular and diffuse intensities in a low-angle rocking curve, their ratio denoted as Q . Studies of Fe/Cr multilayers grown at different substrate temperatures claimed a correlation of Q with the GMR.¹⁹ Several models were developed for the x-ray scattering from rough multilayers which exhibit the two kinds of roughness mentioned above.^{18,20} In all these models, despite the different functional expressions for Q , a larger Q implies a smaller rms correlated roughness, σ_C . Here, the Q 's for every Bragg peak increase with annealing temperatures up to 300–350°C and particularly that of the second-order Bragg peak [Fig. 4(b)]. According to the models mentioned above, this implies a decrease of the vertically correlated roughness with annealing (offset $\theta-2\theta$ scans proved the existence of correlated roughness to some extent since there is still Bragg peaks with the same periodicity as the specular reflections). Therefore, due to annealing up to 300–350°C the interfaces become *less correlated vertically*, and at the same time *more interdiffused*. Interdiffusion may increase spin-dependent scattering since chromium alloying in the Fe layers is known to enhance GMR.^{21,22} However interdiffusion is an atomic scale “roughness,” therefore on a scale much shorter than the x-ray coherence length. In the absence of detailed structural refinement¹⁵ (which was not possible here) it is hard to make a definite statement regarding the quantitative relations

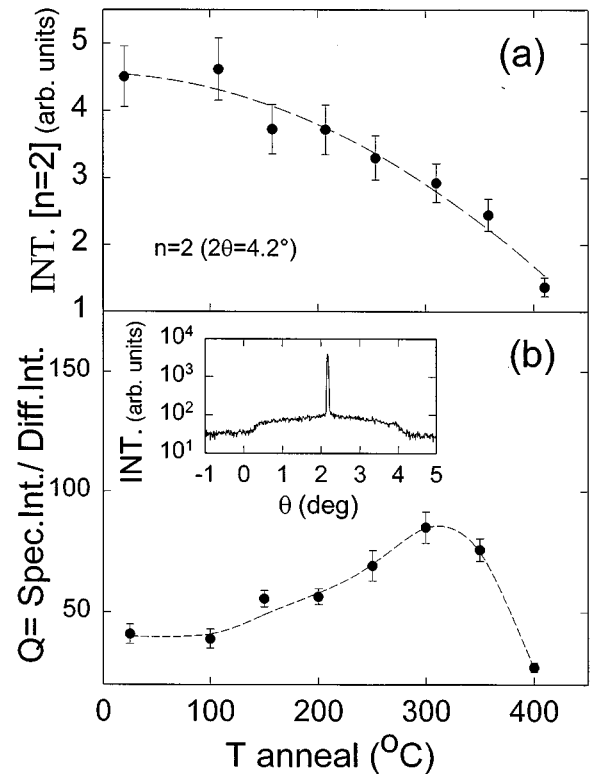


FIG. 4. (a) Intensity of the second-order superlattice Bragg peak over the background intensity for the 12 h annealed samples. (b) Ratio of the specular to diffuse intensity (Q) in the second-order superlattice peak for the 12 h annealed samples. Lines are guides to the eye. The inset shows a rocking curve about a second-order low-angle Bragg peak as an example from which the factors Q were calculated.

between interdiffusion and correlated or uncorrelated roughness. However, since interdiffusion may occur at atomic length scales, interdiffusion is expected to be uncorrelated from layer to layer.

At moderate temperatures, for which $\Delta\rho$ reaches a maximum, the correlated roughness decreases [Fig. 4(b)], while the interdiffusion increases [Fig. 4(a)]. The optimum $\Delta\rho$ is the result of a competition between two mechanisms; an increase in $\Delta\rho$ due to a less correlated interface roughness and/or a moderate interdiffusion, and a decrease in $\Delta\rho$ due to magnetic shorts which drastically lower the AF coupling fraction of the sample. The fact that the spin-dependent scattering at the interface is especially important in the Fe/Cr system²³ further strengthens the arguments presented above.

A similar, although smaller, overall dependence of $\Delta\rho$ on ion dosage was observed in Xe⁺-irradiated Fe/Cr (110) multilayers¹³ (from $\sim 7\%$ to a maximum $\sim 8\%$ at 77 K). Cr alloying of the Fe layer in Fe/Cr(110) can also increase the GMR, from ~ 6.9 to $\sim 12.2\%$.^{21,22} Further comparison is unwarranted since the number of bilayers (cumulative disorder), crystallinity, etc., are different.

In summary, annealing can enhance the GMR in Fe/Cr(110) multilayers, although the annealing temperature range is narrow. Large interdiffusion and bulk crystallinity improvement are generally observed after high-temperature anneals and lead to magnetic shorts, which is detrimental for

GMR. A less correlated interface roughness and/or slight interdiffusion, at moderate temperatures, increases $\Delta\rho$ and therefore the GMR.

We thank T. Ryabtseva for help in the initial stages of this work. We are indebted to Dr. D. Lederman, Dr. R. Schad,

and Dr. P. Belien for a critical reading of the manuscript and useful discussions, and acknowledge financial support from the U.S. Department of Energy. J.M.C. acknowledges the Spanish Secretaría de Estado de Universidades e Investigación.

*Present address: Instituto de Ciencia de Materiales de Madrid-C.S.I.C., Cantoblanco 28049, Madrid, Spain.

¹M. N. Baibich, J. M. Broto, A. Fert, F. Nguyen Van Dau, and F. Petroff, Phys. Rev. Lett. **61**, 2472 (1988).

²S. S. P. Parkin, N. More, and K. P. Roche, Phys. Rev. Lett. **64**, 2304 (1990).

³B. A. Gurney, V. S. Speriosu, J.-P. Nozieres, H. Lefakis, D. R. Wilhoit, and O. U. Need, Phys. Rev. Lett. **71**, 4023 (1993), and references therein.

⁴E. E. Fullerton, M. J. Conover, J. E. Mattson, C. H. Sowers, and S. D. Bader, Phys. Rev. B **48**, 15 755 (1993).

⁵A. Berger, and H. Hopster, Phys. Rev. Lett. **73**, 193 (1994).

⁶S. S. P. Parkin, T. A. Rabedeau, and A. Modak (unpublished).

⁷D. Altbir, M. Kiwi, R. Ramirez, and I. K. Schuller, J. Magn. Magn. Mater. **149**, L246 (1995).

⁸E. E. Fullerton, D. M. Kelly, J. Guimpel, I. K. Schuller, and Y. Bruynseraede, Phys. Rev. Lett. **68**, 859 (1992).

⁹J. Colino, I. K. Schuller, R. Schad, C. D. Potter, P. Belien, G. Verbanck, V. V. Moshchalkov, and Y. Bruynseraede, Phys. Rev. B **53**, 766 (1996).

¹⁰F. Petroff, A. Barthélémy, A. Hamzic, A. Fert, P. Etienne, S. Lequien, and G. Creuzet, J. Magn. Magn. Mater. **93**, 95 (1991).

¹¹N. M. Rensing, A. P. Payne, and B. M. Clemens, J. Magn. Magn. Mater. **121**, 436 (1993).

¹²S. S. P. Parkin, Appl. Phys. Lett. **61**, 1358 (1992).

¹³D. Kelly, I. K. Schuller, V. Korenivski, K. V. Rao, K. K. Larsen, J. Bottiger, E. M. Gyorgy, and R. B. van Dover, Phys. Rev. B **50**, 3481 (1994).

¹⁴H. Nakajima, K. Nonaka, Y. Obi, and H. Fujimori, J. Magn. Magn. Mater. **126**, 176 (1993).

¹⁵I. K. Schuller, Phys. Rev. Lett. **44**, 1597 (1980); W. Sevenhans, M. Gijs, Y. Bruynseraede, H. Homma, and I. K. Schuller, Phys. Rev. B **34**, 5955 (1986); E. E. Fullerton, I. K. Schuller, H. Vanderstraeten, and Y. Bruynseraede, *ibid.* **45**, 9292 (1992).

¹⁶H. Vanderstraeten, D. Neerinck, K. Temst, Y. Bruynseraede, E. E. Fullerton, and I. K. Schuller, J. Appl. Crystallogr. **24**, 571 (1991).

¹⁷J. B. Kortright, J. Appl. Phys. **70**, 3620 (1991).

¹⁸D. E. Savage, J. Kleiner, N. Schimke, Y.-H. Phang, T. Jankowski, J. Jacobs, R. Kariotis, and M. G. Lagally, J. Appl. Phys. **69**, 1411 (1991).

¹⁹P. Belien, R. Schad, C. D. Potter, G. Verbanck, V. V. Moshchalkov, and Y. Bruynseraede, Phys. Rev. B **50**, 9957 (1994).

²⁰R. L. Headrick and J.-M. Baribeau, Phys. Rev. B **48**, 9174 (1993).

²¹N. M. Rensing, and B. M. Clemens, J. Appl. Phys. **76**, 6617 (1994).

²²L. H. Chen, T. H. Tiefel, S. Jin, R. B. Van Dover, E. M. Gyorgy, and R. H. Fleming, Appl. Phys. Lett. **63**, 1279 (1993).

²³M. J. Hall, B. J. Hickey, M. A. Howson, M. J. Walker, J. Xu, D. Greig, and P. Wiser, Phys. Rev. B **47**, 12 785 (1993).